A Three-Stage Channel Estimation Approach for RIS-Aided Millimeter-wave MIMO Systems

Mahmoud Naamani, Didier Le Ruyet, Hmaied Shaiek

A Three-Stage Channel Estimation Approach for RIS-Aided Millimeter-wave MIMO Systems

Mahmoud NAAMANI
CNAM,Cédric Laboratory
Paris, France
mahmoud.naamani@lecnam.net

Didier Le Ruyet
CNAM,Cédric Laboratory
Paris, France
didier.leruyet@lecnam.net

Hmaied SHAIEK
CNAM,Cédric Laboratory
Paris, France
hmaied.shaiek@cnam.fr

***Abstract*—Reconfigurable intelligent surfaces (RIS) is a promising device made up of many passive elements that can control the electromagnetic propagation environment by the adjustment of the phase shifts of the reflecting elements. It is considered as a potential technique to enhance coverage and capacity in future 6G communications. However, channel estimation in a RIS aided MIMO wireless communication system is considered a challenging task due to the passive nature of the RIS which implies that the individual or cascaded channels can be estimated only at the Base Station (BS) or Mobile Station (MS). To address this problem, we proposed a three-stage channel estimation approach where we estimated the channel parameters using compressive sensing (CS). Simulation results showed that the performance of the proposed algorithm is similar to the ones previously proposed as the two-staged approach, but with a lower complexity.**

***Index Terms*—Channel estimation, compressive sensing, millimeter wave, reconfigurable intelligent surface.**

I. Introduction

Reconfigurable intelligent surfaces are considered as the key enablers to improve the coverage of the signal and resolve the frequent blockage in the millimeter wave (mmWave) multiple-input multiple-output (MIMO) communication systems with low hardware cost and energy consumption. It is a planar structure that controls the wireless communication environment by tuning the coefficients of the RIS elements [1] in order to achieve a specific targets, by example focusing the signal towards the receiver [2]. The deployment of the RIS is also accompanied by other benefits, such as improving the physical layer security [3]. The promising performance gain provided by the RIS depends on the accuracy of the acquired channel state information (CSI), where a perfect CSI guarantee an optimal design of the beamforming vectors at the BS,MS, and RIS phase control matrix. The CSI includes the BS-RIS and RIS-MS channels. In [4] the authors studied a RIS aided multi-user MISO downlink communication, where the results showed that the RIS improved the system throughput by around 40%. In [5] through jointly optimizing the RIS reflection coefficients, the fundamental capacity limit of RIS-assisted point-to-point MIMO communication systems was characterized. Results showed that the use of a RIS had increased the capacity of the system. However, it is challenging to acquire the CSI due to the passive nature of the RIS which lacks the ability to transmit, receive or process pilot signals, so channel estimation (CE) can only be done at the level of the BS or MS. As the mmWave MIMO channel is inherently sparse due to the limited number of distinguishable paths, one widely used theory for CE is Compressive Sensing (CS) which takes advantage of this sparsity and estimates the channel with much less pilot overhead. CS is a well-known signal processing technique where a signal that is sparse in a known transform domain could be recovered by much fewer samples than the usually required through finding solutions to under-determined linear systems. In [6] channel estimation is studied for downlink RIS-Aided mmWave MIMO system having multi-antenna base station and mobile station where the authors presented a two-staged iterative re-weighted approach to find the estimates of the channel parameters. In [7] the authors studied a two-staged channel estimation for RIS-Aided mmWave MIMO System via atomic norm minimization.

In this paper we will study CE problem for a passive RIS-aided mmWave MIMO system. Our approach relies on the fact that the channel between the BS and the RIS is static, thus it will not always be estimated. The channel estimation procedure is divided into three stages where we will apply OMP in every stage to estimate the channel parameters. In the first stage we will estimate the angle of departure (AoD) at the BS and consider it known for the rest of the CSI acquisition, then in the second stage and using the estimated angle in the first stage we will estimate the angle of arrival (AoA) at the MS, and in the third stage we will estimate the rest of the channel parameters. Finally we will provide numerical results to validate the performance of our proposed approach.

This paper is organized as follows: Section II introduces the channel model for the RIS-aided mmWave MIMO system, followed by channel estimation procedure in Section III where different CE stages are discussed. Section IV explains the complexity of our algorithm. Section V shows the simulation results, and finally Section VI draws out the conclusion.

Notation: $(.)^H$, $(.)^T$, and $(.)^*$ denote Hermitian trans-

pose, transpose, and conjugate, respectively. Small bold letter denotes a vector, and capital bold letter denotes a matrix. The Hadamard, Kronecker and KhatriRao products between two matrices $\mathbf{A}$ and $\mathbf{B}$ are denoted as $\mathbf{A} \odot \mathbf{B}, \mathbf{A} \otimes \mathbf{B}$, and $\mathbf{A} \lozenge \mathbf{B}$ respectively. $\mathbf{AC} \lozenge \mathbf{BD} = (\mathbf{A} \otimes \mathbf{B})(\mathbf{C} \lozenge \mathbf{D})$. $\mathbf{AC} \otimes \mathbf{BD} = (\mathbf{A} \otimes \mathbf{B})(\mathbf{C} \otimes \mathbf{D})$. The function vec($\mathbf{A}$) creates a vector from matrix $\mathbf{A}$ by stacking its columns.$vec(\mathbf{ACB}) = \left(\mathbf{B^T} \otimes \mathbf{A}\right) vec(\mathbf{C})$. If $\mathbf{C}$ is a diagonal matrix then $vec(\mathbf{ACB}) = \left(\mathbf{B^T} \lozenge \mathbf{A}\right) \tilde{\mathbf{c}}$ where $\tilde{\mathbf{c}}$ is a vector holding the diagonal of $\mathbf{C}$. vec($\mathbf{B}$) returns the vectorized form of the matrix $\mathbf{B}$ where vec($\mathbf{B}$)=$\mathbf{b}$. $\mathbf{B}^\dagger$ represent the pseudo-inverse of matrix $\mathbf{B}$

II. Channel Model

We consider a downlink RIS-aided mmWave MIMO system which comprises one multi-antenna BS having N_{BS} antenna elements, one multi-antenna MS having N_{MS} antenna elements, and a RIS having N_{RIS} elements as shown in Fig. 1. In our case we considered that the channel between the BS and RIS is static, supposing that we have a static BS and RIS with no mobility and mobile environment for the channel between the RIS and MS. This implies that $\mathbf{H_{B,R}}$ will not always be estimated in the CE phase. For simplicity we considered that the direct link between the BS and the MS is blocked. Assuming a geometric channel model, $\mathbf{H_{B,R}}$ represents the channel between the BS and the RIS, $\mathbf{H_{R,M}}$ represents the channel between the RIS and the MS, and $\mathbf{\Omega}$ represents the RIS phase control matrix. $\mathbf{H_{B,R}} \in \mathbb{C}^{N_{RIS} \times N_{BS}}$ is defined as:

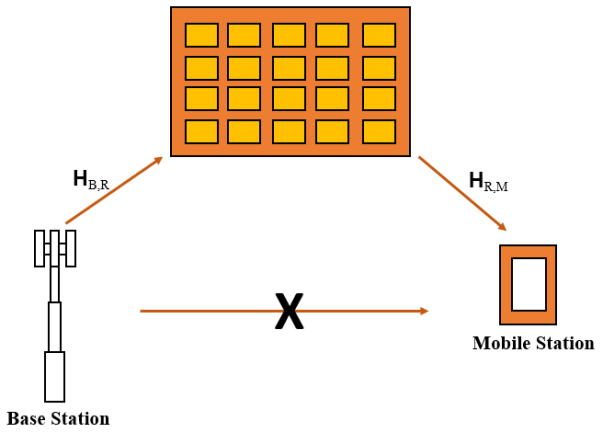

Fig. 1. Down-Link Channel Model

$$\begin{aligned}\mathbf{H_{B,R}} &= \sum_{l=1}^{l_{B,R}} \left[\boldsymbol{\rho}_{B,R}\right]_l \boldsymbol{\alpha_R}\left(\omega_{A,RIS}\right)_l \boldsymbol{\alpha_B}^H \left(\omega_{D,BS}\right)_l \\ &= \mathbf{A_R}\left(\omega_{A,RIS}\right) diag\left(\boldsymbol{\rho}_{B,R}\right) \mathbf{A_B}^H \left(\omega_{D,BS}\right) \\ &= \mathbf{A_R}\left(\omega_{A,RIS}\right) \boldsymbol{\rho}_B \mathbf{A_B}^H \left(\omega_{D,BS}\right) \end{aligned} \quad (1)$$

With $\boldsymbol{\rho}_B = diag\left(\boldsymbol{\rho}_{B,R}\right)$. $\omega_{A,RIS(l)}$ and $\omega_{D,BS(l)}$ denote the AoA at the RIS and the AoD at the BS for the l^{th} path respectively, $\boldsymbol{\rho}_{B,R}$ represents the propagation path gain for the l^{th} path, and $l_{B,R}$ is the number of resolvable paths of the channel. $\mathbf{A_R}\left(\omega_{A,RIS}\right) = \left[\boldsymbol{\alpha_R}\left(\omega_{A,RIS}\right)_1, ..., \boldsymbol{\alpha_R}\left(\omega_{A,RIS}\right)_{l_{B,R}}\right]$, $\alpha_R\left(\omega_{A,RIS}\right)_l, \in \mathbb{C}^{N_{RIS} \times 1}$ is the array response vector for the l^{th} path where $\alpha_R\left(\omega_{A,RIS}\right)_l = e^{j2\pi \frac{d}{\lambda_c}(k-1)sin(\omega_{A,RIS(l)})}$ for $k = 1.....N_{RIS}$, similarly $\boldsymbol{\alpha_B}\left(\omega_{D,BS}\right)_l = e^{j2\pi \frac{d}{\lambda_c}(k-1)sin(\omega_{D,BS(l)})} \in \mathbb{C}^{N_{BS} \times 1}$ where d is the antenna element spacing and λ_c is the carrier wavelength $\mathbf{H_{R,M}} \in \mathbb{C}^{N_{MS} \times N_{RIS}}$ is similarly derived :

$$\begin{aligned}\mathbf{H_{R,M}} &= \sum_{l=1}^{l_{R,M}} \left[\boldsymbol{\rho}_{R,M}\right]_l \boldsymbol{\alpha_M}\left(\omega_{A,MS}\right)_l \boldsymbol{\alpha}_R^H \left(\omega_{D,RIS}\right)_l \\ &= \mathbf{A_M}\left(\omega_{A,MS}\right) diag\left(\boldsymbol{\rho}_{R,M}\right) \mathbf{A}_R^H \left(\omega_{D,RIS}\right) \\ &= \mathbf{A_M}\left(\omega_{A,MS}\right) \boldsymbol{\rho}_R \mathbf{A}_R^H \left(\omega_{D,RIS}\right) \end{aligned} \quad (2)$$

With $\boldsymbol{\rho}_R = diag\left(\boldsymbol{\rho}_{R,M}\right)$. The composite channel $\mathbf{H} \in \mathbb{C}^{N_{MS} \times N_{BS}}$ between the BS and MS through the RIS is expressed as:

$$\begin{aligned}\mathbf{H} &= \mathbf{H_{R,M}} \mathbf{\Omega} \mathbf{H_{B,R}} \\ &= \mathbf{A_M}\left(\omega_{A,MS}\right) \mathbf{G} \mathbf{A_B}^H \left(\omega_{D,BS}\right) \end{aligned} \quad (3)$$

Where $\mathbf{G} = \boldsymbol{\rho}_R \mathbf{A}_R^H \left(\omega_{D,RIS}\right) \mathbf{\Omega} \mathbf{A_R}\left(\omega_{A,RIS}\right) \boldsymbol{\rho}_B \in \mathbb{C}^{l_{R,M} \times l_{B,R}}$ and $\mathbf{\Omega} \in \mathbb{C}^{N_{RIS} \times N_{RIS}}$ is the phase control matrix at the RIS. In this work we assume that two phase shifts are possible $\{0, \pi\}$, so $\mathbf{\Omega}$ which is a diagonal matrix is designed for the training phase based on Hadamard matrix [8]- [9].

III. Channel Estimation Procedure

Assuming that the channel suffers from block fading, for the sounding procedure one coherence time interval is divided into two sub-intervals, the first is for CE and the second for data transmission. All channel parameters remains constant within one coherence time. In our proposal, due to the static nature of $\mathbf{H_{B,R}}$ $\omega_{D,BS(l)}$ will be estimated once within stage 1. Stage 2 and 3 will be repeated periodically to estimate the remaining parameters as shown in Fig. 2.

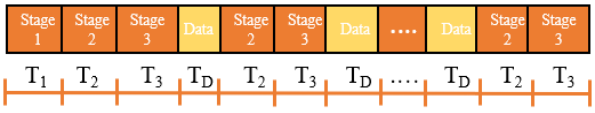

Fig. 2. Sounding and CE procedure

For the channel estimation procedure the BS sends $T = T_1 + T_2 + T_3$ pilots ; $\mathbf{x_t} \in \mathbb{C}^{N_{BS} \times 1}$, $t = 1, ...T$, which will be reflected by the RIS through a phase control matrix $\mathbf{\Omega_t}$ and will be received by the MS. At the MS we have the received signal $\mathbf{y_t} \in \mathbb{C}^{N_{MS} \times 1}$ as:

$$\begin{aligned}\mathbf{y_t} &= \sqrt{P}\mathbf{H}\mathbf{x_t} + \mathbf{n_t} \\ &= \sqrt{P}\mathbf{H_{R,M}}\mathbf{\Omega_t}\mathbf{H_{B,R}}\mathbf{x_t} + \mathbf{n_t} \end{aligned} \quad (4)$$

P is the transmit power and $\mathbf{n}_t$ denotes the additive noise or interference.

A. First Stage

For the first stage, we assume that the BS sends N_{BS} x T_1 matrix of pilot data; $\mathbf{x_t} \in \mathbb{C}^{N_{BS}\times 1}$, $t = i_1, ...T_1$ with $i_1 = 1$, while the RIS holds a fixed reflection pattern $\mathbf{\Omega}_1$. The received signal at the MS is expressed as the following:

$$\mathbf{y_t} = \sqrt{P}\mathbf{H_{R,M}}\mathbf{\Omega}_1\mathbf{H_{B,R}}\mathbf{x_t} + \mathbf{n_t} \tag{5}$$

Now stacking $\mathbf{y_t}$ as $\mathbf{Y_1} = [\mathbf{y_{i_1}}, ...\mathbf{y_{T_1}}]$, $\mathbf{x_t}$ as $\mathbf{X_1} = [\mathbf{x_{i_1}}, ...\mathbf{x_{T_1}}]$, and $\mathbf{n_t}$ as $\mathbf{N_1} = [\mathbf{n_{i_1}}, ...\mathbf{n_{T_1}}]$ we get:

$$\begin{aligned}\mathbf{Y_1} &= \sqrt{P}\mathbf{H}\mathbf{X_1} + \mathbf{N_1} \\ &= \sqrt{P}\mathbf{H_{R,M}}\mathbf{\Omega}_1\mathbf{H_{B,R}}\mathbf{X_1} + \mathbf{N_1} \\ &= \sqrt{P}\mathbf{A_M}\left(\omega_{A,MS}\right)\boldsymbol{\rho}_R\mathbf{A}_R^H\left(\omega_{D,RIS}\right) \\ &\mathbf{\Omega}_1\mathbf{A_R}\left(\omega_{A,RIS}\right)\boldsymbol{\rho}_B{\mathbf{A_B}}^H\left(\omega_{D,BS}\right)\mathbf{X_1} + \mathbf{N_1} \\ &= \sqrt{P}\mathbf{A_M}\left(\omega_{A,MS}\right)\mathbf{G}_1{\mathbf{A_B}}^H\left(\omega_{D,BS}\right)\mathbf{X_1} + \mathbf{N_1}\end{aligned} \tag{6}$$

Where $\mathbf{G}_1 = \boldsymbol{\rho}_R\mathbf{A}_R^H\left(\omega_{D,RIS}\right)\mathbf{\Omega}_1\mathbf{A_R}\left(\omega_{A,RIS}\right)\boldsymbol{\rho}_B$. To obtain $\hat{\omega}_{D,BS(l)}$ the estimate of $\omega_{D,BS_{(l)}}$, we reformulated (6) as an Angle of Arrival estimation problem as following:

$$\begin{aligned}\mathbf{Y_1}^{'} &= \mathbf{X_1}\mathbf{Y_1^H} \\ &= \sqrt{P}\mathbf{A_B}\left(\omega_{D,BS}\right)\mathbf{G}_1^H{\mathbf{A_M}}^H\left(\omega_{A,MS}\right) + \mathbf{X_1}\mathbf{N_1^H} \\ &= \sqrt{P}\mathbf{A_B}\left(\omega_{D,BS}\right)\mathbf{S} + \mathbf{X_1}\mathbf{N_1^H}\end{aligned} \tag{7}$$

where $\mathbf{S} = \mathbf{G}_1^H{\mathbf{A_M}}^H\left(\omega_{A,MS}\right)$. $\omega_{D,BS(l)}$ could be recovered by applying any CS or AoA estimation algorithms on (7). In our case we applied orthogonal matching pursuit (OMP) algorithm to recover $\omega_{D,BS(l)}$, where in order to get a sparse representation of (7) we approximated the array response matrices on a quantized grid as the following:

$$\mathbf{A_B}\left(\omega_{D,BS}\right) \approx \mathbf{A}_{D,BS}\mathbf{Q}_{D,BS} \tag{8}$$

Where:

- $\mathbf{A}_{D,BS}$ is an $N_{BS} \times N_{grid}$ matrix whose columns are the BS array response vectors sampled on a grid of N_{grid} levels corresponding to the possible AoD.
- $\mathbf{Q}_{D,BS}$ is $N_{grid} \times l_{B,R}$ matrix where each column has a single 1 in the position corresponding to $\omega_{D,BS(l)}$

Using (8) we could reformulate (7) as:

$$\begin{aligned}\mathbf{Y_1}^{'} &\approx \sqrt{P}\mathbf{A}_{D,BS}\mathbf{Q}_{D,BS}\mathbf{S} + \mathbf{X_1}\mathbf{N_1^H} \\ &\approx \sqrt{P}\mathbf{A}_{D,BS}\mathbf{C} + \mathbf{X_1}\mathbf{N_1^H}\end{aligned} \tag{9}$$

With $\mathbf{C} = \mathbf{Q}_{D,BS}\mathbf{S}$. Assuming that $N_{B,S} \gg l_{B,R}$, the matrix $\mathbf{C_1}$ will be low rank, and exhibits row sparsity, where we could take advantage of this sparsity and apply OMP in order to obtain $\hat{\omega}_{D,BS(l)}$ for $l = 1.....l_{B,R}$.

B. Second Stage

For the second stage, the BS sends N_{BS} x T_2 matrix of pilot data ; $\mathbf{x_t} \in \mathbb{C}^{N_{BS}\times 1}$, $t = i_2, ...T_2$ with $i_2 = T_1 + 1$, while the RIS holds a fixed reflection pattern $\mathbf{\Omega}_2$. The received signal at the MS is:

$$\mathbf{y_t} = \sqrt{P}\mathbf{H_{R,M}}\mathbf{\Omega}_2\mathbf{H_{B,R}}\mathbf{x_t} + \mathbf{n_t} \tag{10}$$

Now stacking $\mathbf{y_t}$ as $\mathbf{Y_2} = [\mathbf{y_{i_2}}, ...\mathbf{y_{T_2}}]$, $\mathbf{x_t}$ as $\mathbf{X_2} = [\mathbf{x_{i_2}}, ...\mathbf{x_{T_2}}]$, and $\mathbf{n_t}$ as $\mathbf{N_2} = [\mathbf{n_{i_2}}, ...\mathbf{n_{T_2}}]$ we get:

$$\mathbf{Y_2} = \sqrt{P}\mathbf{A_M}\left(\omega_{A,MS}\right)\mathbf{G}_2{\mathbf{A_B}}^H\left(\omega_{D,BS}\right)\mathbf{X_2} + \mathbf{N_2} \tag{11}$$

Where $\mathbf{G}_2 = \boldsymbol{\rho}_R\mathbf{A}_R^H\left(\omega_{D,RIS}\right)\mathbf{\Omega}_2\mathbf{A_R}\left(\omega_{A,RIS}\right)\boldsymbol{\rho}_B$. Using $\hat{\omega}_{D,BS(l)}$, the estimate of $\omega_{D,BS(l)}$ for $l = 1.....l_{B,R}$ obtained in the first stage, we can vectorize $\mathbf{Y_2}$ in (11) as:

$$\begin{aligned}\mathbf{y_2}^{'} &= vec(\mathbf{Y_2}) \\ &\approx \sqrt{P}(\mathbf{X_2}^T \otimes \mathbf{I}_{MS})(\mathbf{A_B}^*\left(\hat{\omega}_{D,BS}\right) \otimes \mathbf{A_M}\left(\omega_{A,MS}\right))\mathbf{g}_2 + \mathbf{n_2}\end{aligned} \tag{12}$$

With $\mathbf{n_2} = vec(\mathbf{N_2})$ and $\mathbf{g}_2 = vec(\mathbf{G}_2)$. To apply CS, we need to get a sparse representation of equation (12), for that we approximate the array response matrices on a quantized grid as following:

$$\mathbf{A_M}\left(\omega_{A,MS}\right) \approx \mathbf{A}_{A,MS}\mathbf{Q}_{A,MS} \tag{13}$$

Where:

- $\mathbf{A}_{A,MS}$ is an $N_{MS} \times N_{grid}$ matrix
- $\mathbf{Q}_{A,MS}$ is $N_{grid} \times l_{R,M}$ matrix

Using the approximation in (13), $\mathbf{y_2}^{'}$ in (12) could be written as:

$$\mathbf{y_2}^{'} \approx \sqrt{P}(\mathbf{X_2}^T \otimes I_{MS})(\mathbf{A_B}^*\left(\hat{\omega}_{D,BS}\right) \otimes \mathbf{A}_{A,MS})\mathbf{q} + \mathbf{n_2} \tag{14}$$

where $\mathbf{q} = (\mathbf{I}^*_{l_{BR}} \otimes \mathbf{Q}_{A,MS})\mathbf{g}_2$ is a sparse vector having sparsity $k = l_{B,R}l_{R,M}$, where each non-zero value corresponds to the angle representing $\omega_{A,MS(l)}$. $(\mathbf{A_B}^*\left(\hat{\omega}_{D,BS}\right) \otimes \mathbf{A}_{A,MS})$ is the dictionary containing the quantized angles representing $\omega_{A,MS(l)}$. Applying OMP on (14) we obtain $\hat{\omega}_{A,MS(l)}$ the estimate of $\omega_{A,MS(l)}$ for $l = 1.....l_{R,M}$.

C. Third Stage

In the third stage the BS sends N_{BS} x T_3 matrix of pilot data ; $\mathbf{x_t} \in \mathbb{C}^{N_{BS}\times 1}$, $t = i_3, ...T_3$ with $i_3 = T_1 + T_2 + 1$, and the RIS reflection pattern is varying with block index t .The received signal at the MS is expressed as the following:

$$\begin{aligned}\mathbf{y_t} &= \sqrt{P}\mathbf{H_{R,M}}\mathbf{\Omega}_t\mathbf{H_{B,R}}\mathbf{x_t} + \mathbf{n_t} \\ &= \sqrt{P}\mathbf{A_M}\left(\omega_{A,MS}\right)\mathbf{G}_t{\mathbf{A_B}}^H\left(\omega_{D,BS}\right)\mathbf{x_t} + \mathbf{n_t} \\ &= \sqrt{P}(\mathbf{x_t}^T \otimes I_{MS})(\mathbf{A_B}^*\left(\omega_{D,BS}\right) \otimes \mathbf{A_M}\left(\omega_{A,MS}\right))\mathbf{g}_t + \mathbf{n_t}\end{aligned} \tag{15}$$

With $\mathbf{g_t} = vec(\mathbf{G_t})$. Using $\hat{\omega}_{D,BS(l)}$ for $l = 1.....l_{B,R}$ and $\hat{\omega}_{A,MS(l)}$ for $l = 1.....l_{R,M}$ obtained from the first and second stage, we rewrite $\mathbf{y_t}$ in (15) as:

$$\begin{aligned}\mathbf{y_t} &\approx \sqrt{P}(\mathbf{x_t}^T \otimes I_{MS})(\mathbf{A_B}^*\left(\hat{\omega}_{D,BS}\right) \otimes \mathbf{A_M}\left(\hat{\omega}_{A,MS}\right))\mathbf{g}_t + \mathbf{n_t} \\ &= \mathbf{B_t}\mathbf{g}_t + \mathbf{n_t}\end{aligned} \tag{16}$$

Where $\mathbf{B_t} = \sqrt{P}(\mathbf{x_t}^T \otimes I_{MS})(\mathbf{A_B}^*\left(\hat{\omega}_{D,BS}\right) \otimes \mathbf{A_M}\left(\hat{\omega}_{A,MS}\right))$. Assuming that we obtained an accurate

estimate of $\omega_{D,BS(l)}$ and $\omega_{A,MS(l)}$ in the first and second stages, one can eliminate $\mathbf{B}$ from (16).

$$\mathbf{B_t}^{\dagger}\mathbf{y_t} = \mathbf{g}_t + \mathbf{B_t}^{\dagger}\mathbf{n_t} \tag{17}$$

We introduce:

$$\mathbf{Y}_B = \left[\mathbf{B}_{i_3}^{\dagger}\mathbf{y}_{i_3} \;\; .... \;\; \mathbf{B}_{T_3}^{\dagger}\mathbf{y}_{T_3}\right]^T \tag{18}$$

$$\mathbf{N}_B = \left[\mathbf{B}_{i_3}^{\dagger}\mathbf{n}_{i_3} \;\; .... \;\; \mathbf{B}_{T_3}^{\dagger}\mathbf{n}_{T_3}\right]^T \tag{19}$$

$$(\mathbf{Y}_B) = \left[\widetilde{\mathbf{\Omega}}_{i_3}.....\widetilde{\mathbf{\Omega}}_{T_3}\right]^T \left[\mathbf{A}_R^T(\omega_{A,RIS}) \lozenge \mathbf{A}_R^H(\omega_{D,RIS})\right]^T \boldsymbol{\rho}^T + {\mathbf{N}_B}^T \tag{20}$$

With $\boldsymbol{\rho} = \boldsymbol{\rho}_B \otimes \boldsymbol{\rho}_R$ and $\widetilde{\mathbf{\Omega}}_t$ is a vector holding the diagonal of $\mathbf{\Omega}_t$. The k^{th} column of $\mathbf{Y}_B$ in (20) is expressed as:

$$(\mathbf{Y}_B)_{:,k} = \left[\widetilde{\mathbf{\Omega}}_{i_3}.....\widetilde{\mathbf{\Omega}}_{T_3}\right]^T \left[\mathbf{A}_R^T(\omega_{A,RIS}) \lozenge \mathbf{A}_R^H(\omega_{D,RIS})\right]^T \boldsymbol{\rho}_{:,k}^T + ({\mathbf{N}_B}^T)_{:,k} \tag{21}$$

Then we approximated the angles at the RIS on a quantized grid as the following:

$$\mathbf{A}_R(\omega_{A,RIS}) \approx \mathbf{A}_{A,RIS}\mathbf{Q}_{A,RIS} \tag{22}$$

$$\mathbf{A}_R(\omega_{D,RIS}) \approx \mathbf{A}_{D,RIS}\mathbf{Q}_{D,RIS} \tag{23}$$

Using (22) and (23), $\mathbf{Y}_B$ in (21) could be approximated as:

$$(\mathbf{Y}_B)_{:,k} \approx \mathbf{\Omega}^{'}\left(\mathbf{A}_{A,RIS}^T \lozenge \mathbf{A}_{D,RIS}^H\right)\mathbf{w}_{:,k} + ({\mathbf{N}_B}^T)_{:,k} \tag{24}$$

Where $\mathbf{\Omega}^{'} = \left[\widetilde{\mathbf{\Omega}}_{i_3}.....\widetilde{\mathbf{\Omega}}_{T_3}\right]^T$, $\mathbf{w} = (\mathbf{Q}_{A,RIS}^T \otimes \mathbf{Q}_{D,RIS}^H)\boldsymbol{\rho}_{:,k}^T$ is a sparse vector where each column represents the k^{th} path, and $(\mathbf{A}_{A,RIS}^T \lozenge \mathbf{A}_{D,RIS}^H)$ is the dictionary containing the quantized angles representing the difference between $\sin(\omega_{D,RIS})$ and $\sin(\omega_{A,RIS})$. The k^{th} column of $[\mathbf{A}_R^T(\omega_{A,RIS}) \lozenge \mathbf{A}_R^H(\omega_{D,RIS})]^T$ could be expressed as

$$\begin{aligned}
&\left([\mathbf{A}_R^T(\omega_{A,RIS}) \lozenge \mathbf{A}_R^H(\omega_{D,RIS})]^T\right)_{:,k} = \\
&= \left([\mathbf{A}_R^T(\omega_{A,RIS}) \lozenge \mathbf{A}_R^H(\omega_{D,RIS})]_{k,:}\right)^T \\
&= \boldsymbol{\alpha_R}(\omega_{A,RIS}) \odot \boldsymbol{\alpha_R}^*(\omega_{D,RIS}) \\
&= e^{j2\pi\frac{d}{\lambda_c}(k-1)(sin(\omega_{A,RIS(l1)}) - sin(\omega_{D,RIS(l2)}))} \\
&= e^{j2\pi\frac{d}{\lambda_c}(k-1)d_{RIS(l)}}
\end{aligned} \tag{25}$$

With $d_{RIS(l)} = sin(\omega_{A,RIS(l1)}) - sin(\omega_{D,RIS(l2)})$ for $l = 1.....l_{B,R}l_{R,M}$, $l_1 = 1.....l_{B,R}$, and $l_2 = 1.....l_{R,M}$.
Applying OMP on every column of (20), we obtain $\hat{d}_{RIS(l)} = sin(\hat{\omega}_{A,RIS(l1)}) - sin(\hat{\omega}_{D,RIS(l2)})$ which represents the difference between the sine of the AoA and AoD at the RIS, and $\hat{\boldsymbol{\beta}}_{(l)}$ which represents the estimation of the product of the propagation path gain $\boldsymbol{\beta}_{(l)} = \boldsymbol{\rho}_{R,M(l1)}\boldsymbol{\rho}_{B,R(l2)}$.

IV. Computational Complexity

Orthogonal Matching Pursuit is an iterative greedy approach that selects at each step the column which is mostly correlated with the current residue. The most computationally intensive steps of OMP are the sweeping stage for choosing the next atom and updating the residue through Least Square (LS). In our complexity analysis we considered only the multiplication operations.
For simplicity, let us consider a simple case of OMP taking into account the following signal:

$$\mathbf{y} = \mathbf{A}\mathbf{u} + \mathbf{n} \tag{26}$$

Where $\mathbf{y} \in \mathbb{C}^{N_{MS}\times 1}$, $\mathbf{A} \in \mathbb{C}^{N_{MS}\times N_{grid}}$ is the dictionary matrix of size N_{grid} , and $\mathbf{u} \in \mathbb{C}^{N_{grid}\times 1}$ is the l-sparse vector. In the k^{th} iteration, the OMP algorithm has a complexity of $\mathcal{O}(N_{grid}N_{MS} + N_{MS}k + N_{MS}k^2 + k^3)$ [10]. In the two-stage approach for the estimation of the AoD and AoA at the BS and MS respectively a dictionary of size N_{grid}^2 is used. In the three stage approach for the estimation of the AoD at the BS a dictionary of size N_{grid} is used and for the estimation of the AoA at the MS a dictionary of size $l_{B,R}N_{grid}$ is used. For the estimation of the angle difference at the RIS and the product of propagation path gain, the dictionary size used is $2N_{grid}$ for both approaches. Since $N_{grid} \gg l_{B,R}$ the complexity in the two-stage approach will be much more higher than the complexity in the three-stage one.

V. Simulation Results

In this section, we evaluated the MSE performance of the parameters estimation in the different stages. The simulation parameters used are as follows: Carrier frequency= 30 GHz, $N_{BS} = N_{MS} = 32, N_{RIS} = 64, l_{B,R} = 1$, and $l_{R,M} = 2$. For quantizing different angles we used a grid having 1.5° resolution. For the first stage we also examined a grid with 0.1° resolution and an adaptive grid where as a first step we used a 1.5° resolution grid then based on the estimated angle $\hat{\omega}$ obtained, we reapplied OMP with a grid resolution of 0.1° for the angle range $\in [\hat{\omega} - 1.5, \hat{\omega} + 1.5]$. The AoD and AoA at the BS, MS, and RIS are generated randomly between $\in \left[0, \frac{\pi}{2}\right]$, $\mathbf{n_t}$ follows $\mathcal{CN}(0, \sigma^2)$, SNR is defined as $\frac{P}{\sigma^2}$, and 4000 realizations are used for averaging. The MSEs of different parameter estimation are defined as:

$$MSE(\omega_{D,BS}) = \frac{\mathbb{E}\left[\sum_{l=1}^{l_{B,R}} \left|\omega_{D,BS(l)} - \hat{\omega}_{D,BS(l)})\right|^2\right]}{l_{B,R}} \tag{27}$$

$$MSE(\omega_{A,MS}) = \frac{\mathbb{E}\left[\sum_{l=1}^{l_{R,M}} \left|\omega_{A,MS(l)} - \hat{\omega}_{A,MS(l)})\right|^2\right]}{l_{R,M}} \tag{28}$$

$$MSE(d_{RIS}) = \frac{\mathbb{E}\left[\sum_{l=1}^{l_{B,R}l_{R,M}} \left|d_{RIS(l)} - \hat{d}_{RIS(l)})\right|^2\right]}{l_{B,R}l_{R,M}} \tag{29}$$

$$MSE(\beta) = \frac{\mathbb{E}\left[\sum_{l=1}^{l_{B,R}l_{R,M}} \left|\beta_{(l)} - \hat{\beta}_{(l)})\right|^2\right]}{l_{B,R}l_{R,M}} \tag{30}$$

The MSE performance of the OMP for different grid resolutions are shown in Fig. 3. A better MSE is obtained with higher grid resolution. Furthermore, the noise error floor decreased with the increase of the grid resolution . The MSE performance of the OMP algorithm for the estimation of the AoD at BS and AoA at MS is shown in Fig 4. The MSE for the estimation of the difference of the sine of the angles at the RIS is shown in Fig 5, and the MSE for the estimation of the product of the propagation path gain is shown in Fig 6. As benchmark, we provide the two-stage channel estimation approach in [6]. Simulation results showed that for the estimation of the AoD at BS and the AoA at MS we have reached almost the same performance in the three-stage channel estimation approach compared to the two-stage approach for a grid resolution of $1.5°$, as same MSE is obtained. A small error is observed between the two-stage and three-stage approaches as in the two-stage the best pair is chosen for the AoD at BS and the AoA at MS, whereas in the three-stage algorithm the AoA is estimated based on the AoD obtained from the previous stage. Almost the same results are obtained for the recovery of the difference between the AoA and AoD at the RIS, but with a small error for the same reason explained above. For the estimation of the product of the propagation path gain, simulation results showed also almost the same results for both approaches. However, the advantage gained in the three-stage approach is on the complexity side as shown in Section IV. Simulation results also showed that when using an adaptive grid of $1.5°$ then refining it to $0.1°$ we were able to reach the same performance as using a fixed grid with $0.1°$ resolution, which leaves an option to optimize our algorithm for future work.

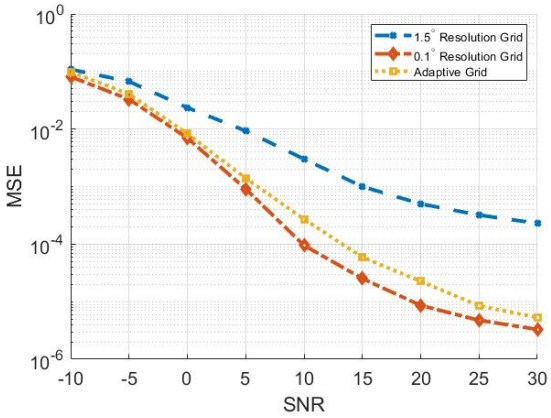

Fig. 3. AoD estimation for different grid resolution

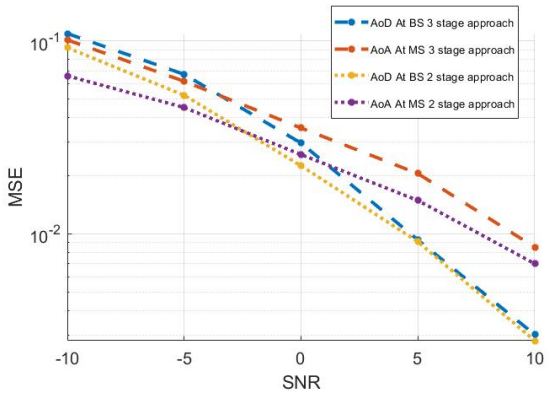

Fig. 4. AoD and AoA estimation at the BS and MS respectively

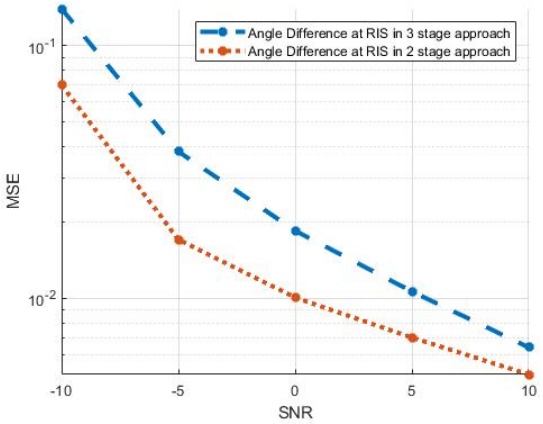

Fig. 5. Angular difference estimate at the RIS

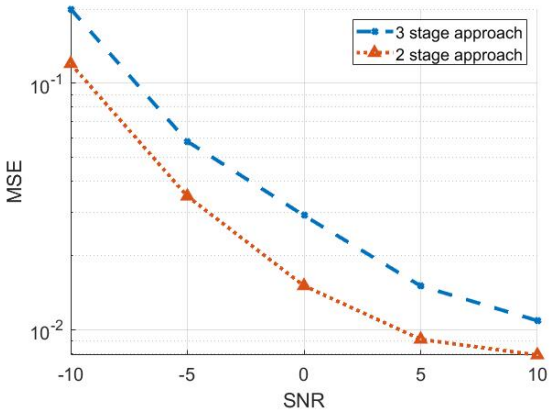

Fig. 6. Product of propagation path gain

VI. Conclusion

We studied the CE problem for the RIS-aided mmWave MIMO systems. We proposed a three-stage approach where we applied compressive sensing to estimate the channel parameters. Simulation results showed that our proposed approach reached the same performance as the two-stage previously proposed, but the advantage of splitting the channel estimation procedure into three steps is clearly seen in terms of the complexity of the algorithm.

References

[1] Yuanwei Liu, Xiao Liu, Xidong Mu, Tianwei Hou, Jiaqi Xu, Marco Di Renzo, and Naofal Al-Dhahir. Reconfigurable intelligent surfaces: Principles and opportunities. *IEEE communications surveys & tutorials*, 23(3):1546–1577, 2021.

[2] Shimin Gong, Xiao Lu, Dinh Thai Hoang, Dusit Niyato, Lei Shu, Dong In Kim, and Ying-Chang Liang. Toward smart wireless communications via intelligent reflecting surfaces: A contemporary survey. *IEEE Communications Surveys & Tutorials*, 22(4):2283–2314, 2020.

[3] Limeng Dong and Hui-Ming Wang. Secure mimo transmission via intelligent reflecting surface. *IEEE Wireless Communications Letters*, 9(6):787–790, 2020.

[4] Chongwen Huang, Alessio Zappone, Mérouane Debbah, and Chau Yuen. Achievable rate maximization by passive intelligent mirrors. In *2018 IEEE International Conference on Acoustics, Speech and Signal Processing (ICASSP)*, pages 3714–3718. IEEE, 2018.

[5] Shuowen Zhang and Rui Zhang. Capacity characterization for intelligent reflecting surface aided mimo communication. *IEEE Journal on Selected Areas in Communications*, 38(8):1823–1838, 2020.

[6] Jiguang He, Markus Leinonen, Henk Wymeersch, and Markku Juntti. Channel estimation for ris-aided mmwave mimo systems. In *GLOBECOM 2020-2020 IEEE Global Communications Conference*, pages 1–6. IEEE, 2020.

[7] Jiguang He, Henk Wymeersch, and Markku Juntti. Channel estimation for ris-aided mmwave mimo systems via atomic norm minimization. *IEEE Transactions on Wireless Communications*, 20(9):5786–5797, 2021.

[8] Zhengyi Zhou, Ning Ge, Zhaocheng Wang, and Lajos Hanzo. Joint transmit precoding and reconfigurable intelligent surface phase adjustment: A decomposition-aided channel estimation approach. *IEEE transactions on communications*, 69(2):1228–1243, 2020.

[9] Changsheng You, Beixiong Zheng, and Rui Zhang. Channel estimation and passive beamforming for intelligent reflecting surface: Discrete phase shift and progressive refinement. *IEEE Journal on Selected Areas in Communications*, 38(11):2604–2620, 2020.

[10] Bob L Sturm and Mads Græsbøll Christensen. Comparison of orthogonal matching pursuit implementations. In *2012 Proceedings of the 20th European Signal Processing Conference (EUSIPCO)*, pages 220–224. IEEE, 2012.